An Investigation of Recent Observed Changes in the Earth's Oblateness

R. S. Nerem, E. W. Leuliette, J. S. Parker (Colorado Center for Astrodynamics Research, University of Colorado, Boulder, CO, 80309, USA, nerem@colorado.edu)
R. S. Gross (Jet Propulsion Laboratory, Pasadena, CA, USA)
A. Cazenave and J. M. Lemoine (GRGS/CNES, 18 Av. E. Belin, 31400 Toulouse, France)
D. P. Chambers (Center for Space Research, The University of Texas at Austin, Austin, TX, 78712, USA)

Abstract

Beginning in 1998, large changes in the Earth's oblateness have been recently detected using Satellite Laser Ranging (SLR). These changes are consistent with mass moving from the higher latitudes into the equatorial region, and are the largest such changes observed since SLR started tracking the phenomena in the late 1970s. We have conducted a comprehensive investigation into the source of these changes. We have compared SLR results from several different research groups, and concluded there is no problem with the data analysis. We have considered a variety of possible geophysical sources including tide modeling errors, atmospheric mass redistribution, and ocean mass redistribution. Of these, the ocean appears to be the most likely source of the observed oblateness changes. Specifically, the changes appear to be concentrated in the Pacific Ocean. The observed oblateness variations are highly correlated with the Pacific Decadal Oscillation (PDO). We investigated the mass variations in the oceans using two different sources: 1) the ECCO ocean model, and 2) TOPEX/Poseidon sea level measurements corrected for steric sea level change using buoy observations. These results explain a significant fraction of the observed oblateness changes, but are somewhat smaller in magnitude.

GSFC's Analysis and Results

The motivation for our work stemmed from the SLR data analysis performed by Cox and Chao (2002) at Goddard Space Flight Center. Using SLR data from 10 satellites, including data from Lageos-1, Starlette, Ajisai, Lageos-2, and TOPEX/Poseidon (T/P), over a period from 1979 to 2002, Cox and Chao calculated a surprising ΔJ_2 time series for the Earth. Figures 1-3 summarize the change in the Earth's oblateness from some nominal value over time ($\Delta J_2(t)$) calculated from the SLR data. The dominant feature in Figure 1 is a seasonal signal of amplitude 3.2 x 10^{-10}, driven by meteorologic mass redistribution in the global system. Prior to 1996, a linear fit describes a trend in the observed J_2 of -2.8 x 10^{-11}/year with an uncertainty on the order of 0.4 x 10^{-11}/year. This trend is typically attributed to postglacial rebound and other secondary contributions of climatic and anthropogenic origin, e.g., reservoirs. After 1997, a linear fit of the data results in a J_2 rate of +2.2 x 10^{-11}/year with an uncertainty on the order of 0.7 x 10^{-11}/year.

Our study has analyzed several models, including an atmospheric model by NCEP, the National Center for Environmental Prediction, an ocean model from the consortium ECCO, Estimating the Circulation and Climate of the Ocean, and T/P sea surface height (SSH) measurements with and without a steric model removed.

Satellite Laser Ranging

SLR data, shown in Figure 1, indicate a shift in the change of the Earth's oblateness over time. It is assumed that prior to 1980, up until about 1997, the value of J_2 dot has been roughly constant at -2.8 x 10^{-11}/year. It is apparent that since 1998, $J_2(t)$ has accelerated by some unknown mechanism. Figure 1 shows the Goddard SLR ΔJ_2 time series, Figure 2 shows the data with seasonal terms removed, and Figure 3 shows the data smoothed over 6 months with a trend of -2.8 x 10^{-11}/year removed.

Figure 1. Observed variations in J_2 calculated using SLR data.

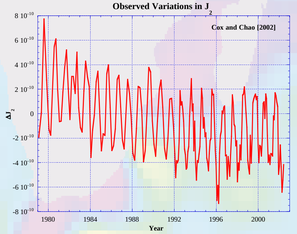

Figure 2. SLR ΔJ_2 Time Series with seasonal terms removed.

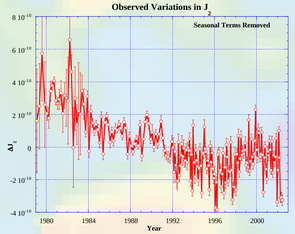

Figure 3. SLR ΔJ_2 Time Series: seasonal terms removed; rate of -2.8 x 10^{-11}/year removed; 6-month smoothing applied.

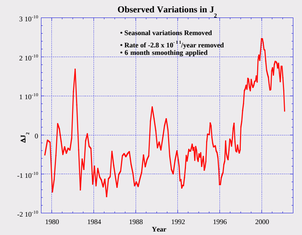

NCEP Model

The National Center for Environment Prediction (NCEP) produced ΔJ_2 time series, computed from the harmonic coefficients of the NCEP reanalysis surface pressure fields supplied by the IERS Special Bureau for the Atmosphere at AER. Figure 4 compares the NCEP ΔJ_2 time series with the SLR ΔJ_2 time series.

Figure 4. Comparison of the NCEP ΔJ_2 time series with the SLR ΔJ_2 time series.

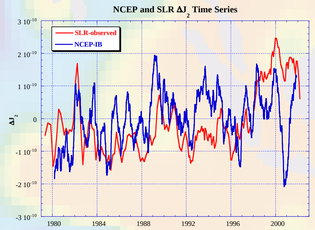

Squared coherency values were computed for the NCEP model ΔJ_2 time series compared with the GSFC ΔJ_2 time series, displayed in Figure 5.

Figure 5. Squared Coherency Plots: SLR & NCEP ΔJ_2 time series.

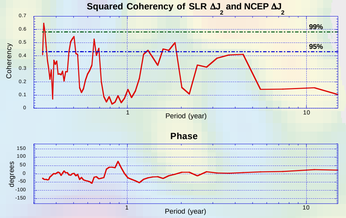

As seen in Figure 5, there is overall coherency strength between the SLR ΔJ_2 time series and the NCEP ΔJ_2 time series at periods from 1.25 years to about 5 years. Furthermore, the two time series are nearly in-phase in that range of periods. This suggests that the atmosphere can be used to help predict J_2 at interannual periods.

Comparing with the Pacific Decadal Oscillation (PDO)

Figures 6 and 7 show how Cox and Chao's ΔJ_2 time series compares with the Pacific Decadal Oscillation (PDO). This comparison suggests that a substantial part of the global change in J_2 may be attributed to the Pacific Ocean fluctuations.

Figure 6. Comparison of the SLR ΔJ_2 Time Series with the PDO.

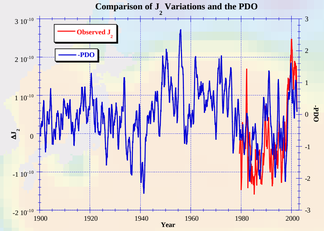

Figure 7. Comparison of ΔJ_2 and PDO, each with 6-month smoothing applied.

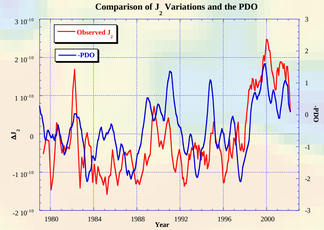

The features of the Pacific Decadal Oscillation, seen in Figure 7, correlate fairly well with the SLR time series, suggesting that the Pacific Ocean may be responsible for the observed change in J_2.

Squared coherency values were computed for the PDO time series compared with the SLR ΔJ_2 time series, displayed in Figure 8.

Figure 8. Squared Coherency Plots: PDO and SLR ΔJ_2 time series.

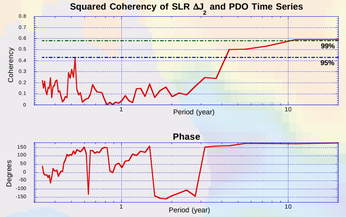

As seen in Figure 8, there is significant coherency between the two time series at periods greater than five years. The two time series are very nearly 180 degrees out of phase at the strongest coherencies, which is as expected since the SLR ΔJ_2 time series was being compared with the negative PDO time series. Hence, the long-scale features are very similar in the two time series, suggesting that the Pacific Decadal Oscillation may reflect the global J_2 over long periods.

18.6-Year Tide?

We attempted to adjust J_2 dot and the 18.6 and 9.3 year tides to reduce the size of the J_2 anomaly, the results of which are shown in the following table. While it is possible to nearly completely eliminate the J_2 anomaly in this way, the solutions for these parameters are unrealistic. J_2 dot changes to -1.7 x 10^{-11}/year, and the phase of the 18.6 year tide changes from its equilibrium value by more than 20 degrees. In addition, these values are substantially different from those obtained from data covering only the 1980-1996 time period, as shown in the table.

Solutions for J_2 Fits

Solution	18.6 Amplitude	18.6 Phase	9.3 Amplitude	J_2 dot x 10^{-11}/year
GSFC Nominal	0.63 cm	0°	0.0 cm	-2.8
Adjust 18.6	0.53 cm	28°	0.0 cm	-2.8
Adjust 18.6 and 9.3	0.49 cm	21°	0.24 cm	-2.8
Adjust 18.6 and J_2 dot	0.71 cm	23°	0.0 cm	-1.7
Adjust 18.6, 9.3, and J_2 dot	0.66 cm	18°	0.21 cm	-1.8
Adjust 18.6, 9.3, and J_2 dot (1980-1996)	0.58 cm	4°	0.11 cm	-2.6

Grey Shading = not adjusted in solution, fixed at "nominal" values

ECCO Model

A ΔJ_2 time series has been obtained using the ECCO ocean model by integrating the ocean density field throughout the volume of the modeled ocean [Stammer et al., 2002]. The model spans 1980-2001 using surface heat flux and evaporation-precipitation fields from the NCEP/NCAR reanalysis project. From 1993-2001, it also assimilates T/P SSH data. ECCO uses the oceanic general circulation model developed by Marshall et al. [1997a, 1997b], which employ Boussinesq approximations. Since Boussinesq approximations conserve volume rather than mass, artificial mass variations may be introduced into the model depending on the applied surface heat and salt fluxes. Mass conservation was restored to the model by adding a uniform layer to the modeled sea surface of just the right time-dependent thickness [Greatbatch, 1994; Greatbatch et al., 2001]. The effect of this mass-conserving layer is included in each of the ECCO model plots.

Global Study:

A global ΔJ_2 time series was computed using the ECCO model's ocean bottom pressure (OBP) data converted into height. Figure 9 compares the ECCO model results with the ΔJ_2 time-series produced by Cox & Chao.

Figure 9. ECCO OBP ΔJ_2 time series compared with Cox and Chao's SLR ΔJ_2 time series.

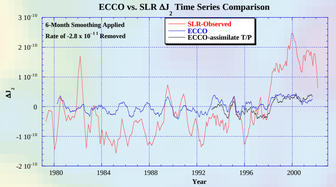

Squared coherency values were computed for the ECCO model OBP ΔJ_2 time series compared with the SLR ΔJ_2 time series, displayed in Figure 10.

Figure 10. Squared Coherency Plots: SLR & ECCO ΔJ_2 time series.

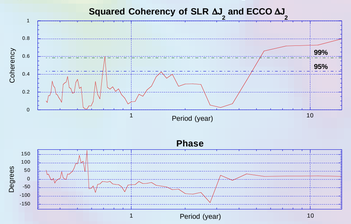

As seen in Figure 10, there is significant coherency between the two time series at periods greater than five years. Hence, the long-scale features are very similar in the two time series, suggesting that the ECCO ocean model can predict J_2 to some degree over long periods. One can also see that the SLR ΔJ_2 and the ECCO ΔJ_2 are nearly in phase where the coherency is significant.

Empirical Orthogonal Function (EOF) Analysis:

An EOF analysis was performed on the global ocean bottom pressure data produced by the ECCO model. Figure 11 displays the first four EOF modes and their time series, comprising roughly 77.4% of the data when the sum is taken of these four modes multiplied by their respective time series.

Figure 11. Global OBP EOF Modes 1-4 (in cm) and respective time series, with ΔJ_2 time series shown below.

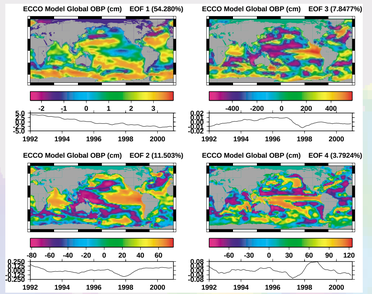

As seen in Figure 11, the first EOF mode holds mostly a secular trend; modes 2 and 3 contain information reflecting El Nino.

Global T/P SSH

TOPEX/Poseidon sea surface height data from December, 1992 to April, 2002 has been collected and analyzed using an EOF analysis to generate the most significant modes' ΔJ_2 time series. Figure 12, below, displays the first four modes of the EOF decomposition and their respective time series, produced from the global oceans. Roughly 55.8% of the spatial and temporal data can be reconstructed by these four modes. The J_2 constituents were calculated in each of the modes' spatial maps and ΔJ_2 time series were constructed as shown at the bottom of the figure.

Figure 12. T/P Global SSH EOF Analysis, Modes 1-4 and their time series (cm). Corresponding ΔJ_2 time series shown below.

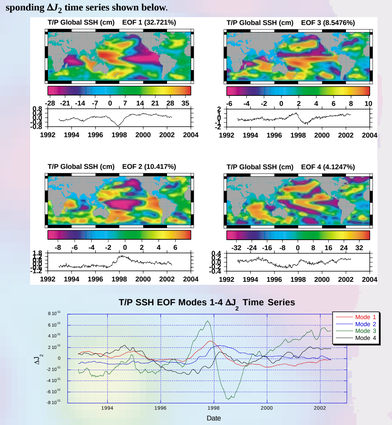

T/P SSH and XBT Model

TOPEX/Poseidon altimetry data from January, 1993 to December, 2001 have been used to produce a ΔJ_2 time series for the global oceans and for the Pacific Ocean alone. In order to study the interannual variations in the ocean mass, a steric model of the oceans must be removed. The model used in this study took advantage of subsurface temperature measurements made by temperature recorders, such as expendable bathythermographs (Sets), to measure the thermal portion of the steric signal [Chambers et al., 2000].

The XBT data were interpolated using a five-degree Gassing weighted smoother to a uniform 5° grid. Empirical Orthogonal Function reconstruction was performed to fill in any data gaps. A gridded resolution of five degrees is sufficient to detect degree/order 2 variations; it is also better suited to fill in gaps and to reduce problems with eddies. The monthly global steric correction was then removed from the mean sea level variation determined by T/P altimetry. The inverted barometer correction was not included in the T/P data.

Figure 13, below, displays the ΔJ_2 time series constructed from each of the three grids: T/P SSH, XBT map, and the residuals from the T/P SSH minus the XBT grid.

Figure 13. The ΔJ_2 time series corresponding to the T/P SSH spatial map, the XBT filled spatial map, and the map of the T/P - XBT residuals.

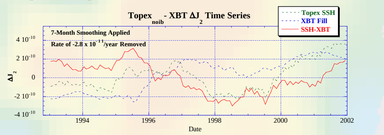

The results of the global T/P SSH - XBT model show a ΔJ_2 time series of the same order of magnitude as the SLR ΔJ_2 time series. The ΔJ_2 time series shown below in Figure 14 was produced from a 5° map of the T/P SSH - XBT residuals in the northern Pacific Ocean only. Looking only at the northern Pacific Ocean, representative of the Pacific Decadal Oscillation, the magnitude of the ΔJ_2 time series is not large enough to account for the global SLR ΔJ_2 time series.

Figure 14. The ΔJ_2 time series of the T/P SSH - XBT residuals in the Northern Pacific Ocean.

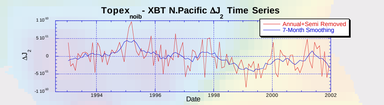

Discussion

We have investigated the source of a large change in J_2 which began in 1998 [Cox and Chao, 2002]. Figure 15, below, compares the influence of the atmosphere and the oceans on the J_2 time series with the SLR observations of $\Delta J_2(t)$.

Figure 15. A comparison on the influence of the atmosphere and oceans on the observed SLR ΔJ_2 time series.

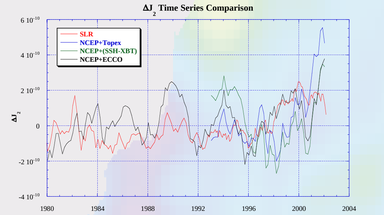

Interannual variations in the atmosphere can account for part of the variation. A large change in the Pacific Ocean beginning in 1998 can account for a significant part of the most recent change. However, part of the change is still unexplained, and thus research on this phenomena will continue.

References

Chambers, D.P., Chen, J., Nerem, S., and Tapley, B.D. 2000, Interannual Mean Sea Level Change and the Earth's Water Mass Budget, *Geophys. Res. Lett.*, **27**, 3073-3076.

Cox, C.M. and Chao, B.F. 2002, Detection of a Large-Scale Mass Redistribution in the Terrestrial System Since 1998, *Science*, **297**, 831-833.

Greatbatch, R.J. 1994, A note on the representation of steric sea level in models that conserve volume rather than mass, *J. Geophys. Res.*, **99**, 12767-12771.

Greatbatch, R.J., Lu, Y., and Cai, Y. 2001, Relaxing the Boussinesq approximation in ocean circulation models, *J. Atmos. Oceanic. Technol*, **18**, 1911-1923.

Marshall, J., Hill, C., Perelman, L., and Adcroft, A. 1997a, Hydrostatic, quasi-hydrostatic, and non-hydrostatic ocean modeling, *J. Geophys. Res.*, **102**, 5733-5752.

Marshall, J., Adcroft, A., Hill, C., Perelman, L., and Heisey, C. 1997b, A finite-volume, incompressible, Navier Stokes model for studies of the ocean on parallel computers, *J. Geophys. Res.*, **102**, 5753-5766.

Stammer, D., Wunsch, C., Fukumori, I., and Marshall, J. 2002, State estimation improves prospects for ocean research, *EOS Trans. Amer. Geophys. Soc.*, **83(27)**, 289-295.

Acknowledgments

Cox and Chao [2002] provided the SLR J_2 time series for this study.